

## Development of the ACSpect neutron spectrometer: Technological advance and response against an accelerator-based neutron beam

Gabriele Parisi<sup>a,b,\*</sup>, Andrea Pola<sup>c,d</sup>, Davide Bortot<sup>c,d</sup>, Davide Mazzucconi<sup>c,d</sup>, Giovanni D'Angelo<sup>c,d</sup>, Chiara Magni<sup>e,f</sup>, Ian Postuma<sup>f</sup>, Silva Bortolussi<sup>e,f</sup>, Nicoletta Protti<sup>e,f</sup>, Saverio Altieri<sup>e,f</sup>, Umberto Anselmi Tamburini<sup>e,f</sup>, Valerio Vercesi<sup>f</sup>, Stefano Agosteo<sup>c,d</sup>

<sup>a</sup> Department of Physics, University of Surrey, Guildford, UK

<sup>b</sup> NPL – National Physical Laboratory, Teddington, UK

<sup>c</sup> Politecnico di Milano, Milan, Italy

<sup>d</sup> INFN – Istituto Nazionale di Fisica Nucleare, sezione di Milano, Milan, Italy

<sup>e</sup> Università di Pavia, Pavia, Italy

<sup>f</sup> INFN – Istituto Nazionale di Fisica Nucleare, sezione di Pavia, Pavia, Italy

### ARTICLE INFO

#### Keywords:

Neutron spectrometer  
Silicon detector  
High resolution neutron spectrometry  
Boron neutron capture therapy

### ABSTRACT

Advances in neutron-based radiation therapies such as Boron Neutron Capture Therapy (BNCT) pushes towards the development of new neutron spectrometers, whose key features are to be their practicability, reliability, energy resolution and detection range. The ACSpect is a novel neutron spectrometer based on a two-stages monolithic silicon telescope detector coupled to an organic scintillator working as an active neutron converter.

This paper reports the latest developments of the ACSpect and the results of the measurements of an accelerator-based neutron beam moderated by  $AlF_3$ . The  $AlF_3$  is a moderator material optimised to obtain an epithermal neutron beam for accelerator-based BNCT of deep seated tumours. The experiments carried out are the first neutron spectrometry of a neutron beam moderated by  $AlF_3$ .

The performances of the ACSpect have been compared against Monte Carlo simulations, literature data and the gold-standard neutron spectrometer DIAMON. While the agreement between experiments and simulations allowed to validate the Monte Carlo model used to simulate the new moderator material, the agreement between literature data, ACSpect and DIAMON results confirmed the ACSpect as a compact and relatively easy-to-use high-resolution neutron spectrometer, capable of reliably operating in the energy range 250 keV - 4 MeV.

### 1. Introduction

Neutron spectrometry is not trivial since these particles ionise matter indirectly and their energy distribution may extend from thermal energies up to hundreds MeV. There are various techniques and devices employed for neutron spectrometry: moderation detectors (e.g. the Bonner Sphere Spectrometer, BSS), recoil-proton detectors, proportional counters, activation techniques, time of flight detectors (ToF), etc. This work describes the use of two different devices to measure the spectrum of an accelerator-based neutron beam.

One is an innovative moderation detector implemented by the nuclear measurements group of Politecnico di Milano in collaboration with Raylab, an Italian start-up spin off of Politecnico di Milano, the Direction-aware Isotropic and Active MONitor with spectrometric

capabilities (DIAMON), (Pola et al., 2020). DIAMON employs a single block of moderator containing several position-sensitive thermal neutron detectors. The response matrix is constituted by the different positions of the thermal neutron detectors, instead of the diameter of the spheres composing a typical BSS. In this way all measurements can be made simultaneously. DIAMON innovative design leads to an isotropic response and to an optimised energy dependence. The embedded proprietary unfolding code *UNCLE* allows a real-time assessment of the neutron spectrum and a subsequent derivation of the spectrum from thermal neutron energies to 20 MeV the low energy version, and to 5 GeV the high energy version.

The other device employed is the ACSpect (*Active Converter Spectrometer*), a recoil proton detector designed and improved at the Politecnico di Milano (Stefano Agosteo et al., 2007, 2016). This high energy

\* Corresponding author. Department of Physics, University of Surrey, Guildford, UK.

E-mail address: [g.parisi@surrey.ac.uk](mailto:g.parisi@surrey.ac.uk) (G. Parisi).

<https://doi.org/10.1016/j.radmeas.2022.106776>

Received 2 June 2021; Received in revised form 19 April 2022; Accepted 29 April 2022

Available online 4 May 2022

1350-4487/© 2022 The Authors. Published by Elsevier Ltd. This is an open access article under the CC BY-NC-ND license (<http://creativecommons.org/licenses/by-nc-nd/4.0/>).

resolution spectrometer is based on a two-stages Monolithic Silicon Telescope (MST) coupled, through a collimator, to an organic scintillator that works as an active converter as well.

The ACSpect was further improved in the framework of this work by modifying its configuration and the whole elaboration process. The result is a much more compact instrument set-up, with better portability and higher adaptability to different experimental environments, being much less sensitive to external disturbances. Notably, the energy resolution achieved by this spectrometer down to 200 keV has otherwise been achieved only by time of flight systems, which are more complex and impossible to transport.

This paper describes the improvement implemented to the ACSpect, comprehensively describing its working principles, and it reports of an experimental campaign carried out at Legnaro National Laboratories. A neutron field obtained by irradiating a beryllium target with 5 MeV protons was characterised by means of the improved ACSpect, both in the free-beam configuration and after crossing some layers of a new moderator material consisting of densified powder of aluminium fluoride ( $\text{AlF}_3$ ). Results were compared with literature data and with measurements carried out with the DIAMON to prove the ACSpect reliability. The spectra measured moderating the beam with the  $\text{AlF}_3$  layers are the first test of the new moderator material and they were used to validate Monte Carlo simulations performed with *MCNP6*.

## 2. Materials & methods

### 2.1. The ACSpect and its improvement

The ACSpect is a recoil-proton neutron spectrometer based on a silicon telescope coupled with a plastic active converter. Fig. 1 shows a scheme of the whole ACSpect. The active converter has the double function of converting impinging neutrons to recoil-protons and measuring their energy distribution. It is a 2 mm thick BC-404 scintillator, based on polyvinyl-toluene, fabricated by Saint-Gobain Crystals (Saint-Gobain Crystalsa; Saint-Gobain Crystalsb), with an overall area of  $7.3 \times 9.5 \text{ mm}^2$ . The scintillator energy-response is non-linear against LET, thus decreasing the light conversion yield. This non-linearity is resolved by an analytical linearization procedure developed by Lorenzoli (Stefano Agosteo et al., 2016), considering the Birk's law to express the non-linearity (John Bettely Birks, 1951; John Bettely Birks et al., 1964). The scintillator is coupled to the H10720-110

photo-multiplier tube fabricated by Hamamatsu (url: [http, 1072](http://1072)). This first part of the spectrometer, consisting of the scintillator coupled to the photo-multiplier, is referred to as PM from here on.

In order to narrow the detectable recoil-proton emission angle span, a cylindrical aluminium collimator, connecting the active converter to the telescope, was designed with a length of 21 mm and a diameter of 4 mm. Using the collimator, only the scintillator area facing the collimator is actually sensitive. Therefore, the scintillator sensitive area is  $12.57 \text{ mm}^2$  leading to a recoil-proton maximum detectable emission angle of  $\theta = 7.35^\circ$  (Stefano Agosteo et al., 2016).

The monolithic silicon telescope (MST) is a semiconductor silicon wafer aligned to the scintillator and placed into a sealed aluminium box put under vacuum (together with the collimator). It is characterised by two stages, commonly referred to as  $\Delta E$  and  $E$ . They are  $1.9 \mu\text{m}$  and  $500 \mu\text{m}$  thick respectively, with a square area of  $1 \text{ mm}^2$ . The two stages behave like two biased  $p$ - $n$  junction diodes collecting charges via drift driven separation of electron-hole pairs in the polarised depletion region. More details about the MST can be found in (Rosenfeld et al., 1999).

By coupling telescope and scintillator events through a time coincidence algorithm, detected neutrons are wholly characterised in energy. Their fluence rate is eventually retrieved through calculations based on cross-section data of the (n,p) reaction in polyvinyl-toluene.

Additional details about the ACSpect components design and its optimisation can be found in (Stefano Agosteo et al., 2007, 2016).

The ACSpect has been improved by innovating its front-end electronics and the data processing program. The spectrometer has eventually been calibrated in its new configuration.

#### 2.1.1. Front-end electronics

The objective of innovating the spectrometer front-end electronics was to decrease its exposure to external disturbances (e.g. electromagnetic disturbances from the particle accelerator) and electronic noise.

Two equal electronic boards were used. Each of them can handle two channels to which test-line and voltage-bias are coupled. One electronic board is used for the  $\Delta E$  - stage only while the other board is connected to the PM and to the  $E$  -stage. The two silicon telescope channels are equipped with analogous amplification systems made up with a Cremat *CR-110-R2* pre-amplifier and a Cremat *CR-200-2*  $\mu\text{s}$  Gaussian shaping amplifier. The silicon telescope is connected in the so called  $\Delta E$ -*E*to

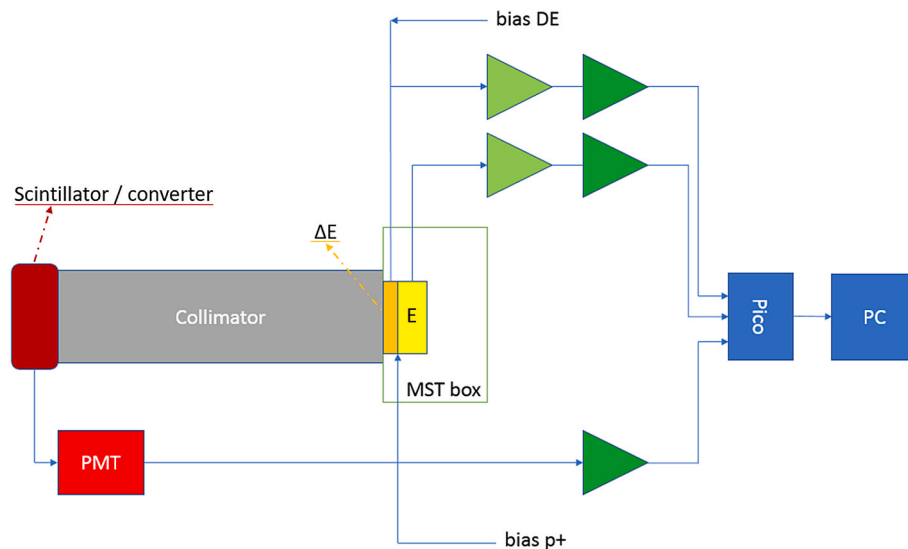


Fig. 1. Scheme of the ACSpect with electronics and acquisition chain. The scheme is not in scale. The dark and light red boxes represent the scintillator/convertor and the photo-multiplier tube, respectively; the orange and yellow boxes represent the  $\Delta E$  and  $E$  stage of the MST, respectively; the dark and light green triangles represent shaping amplifier and pre-amplifier, respectively; the blue box labelled "Pico" represents the acquisition device.

configuration. Hence, the signals coming from its two channels are proportional, respectively, to the charge collected in the thin  $\Delta E$ -stage and to the whole charge deposited in both the first and second stages. The photomultiplier output is directly connected to the amplifier input, since it does not require pre-amplification. In order to accommodate the fast-response and the high count rate of the *PM*, the small-shaping-time amplifier Cremat *CR-200-250ns Gaussian shaping* was chosen.

The whole assembly is placed inside a 122 mm  $\times$  172 mm  $\times$  54 mm aluminium box. Fig. 2 shows the final ACSpect set-up.

It should be stressed that the system is stand-alone and does not need any further equipment other than a multi-channel analyser, bias and power sources. Hence, all external disturbances and noise arising from the use of a classical external amplification chain are reduced strongly.

### 2.1.2. Calibration

An accurate energy calibration of the detector will be performed in the future with quasi-monoenergetic neutrons. An alternative method was used for the time being. Nevertheless, it should be mentioned that the comparison of the measured spectra with literature data and Monte Carlo simulations give confidence with the results discussed herein.

The telescope calibration was performed by using an Am-241 source. Obviously, during the telescope calibration the scintillator had to be removed since otherwise it would have stopped all the alpha particles from the source. Calibration coefficients for  $\Delta E$  and  $E_{tot}$  were assessed found by matching their experimental scatter-plot curve with the theoretical ones, which were calculated with an analytical model (Stefano Agosteo et al., 2016).

Once the telescope has been calibrated with  $\alpha$  particles, the *PM* “self-calibration” was carried out by comparing the *PM* and  $E_{tot}$  spectra, Fig. 3. Since the energy deposited in the scintillator and in the telescope is complementary (the sum is the total recoil-proton energy) they must have the same edge, corresponding to those recoil-protons releasing all their energy within the *PM* or within the telescope. The two edges should superimpose and correspond to the maximum recoil-proton energy. It should be remembered that this calibration method is not as accurate as the use of a calibrated source of quasi-monoenergetic neutrons. The uncertainty of the *PM* calibration coefficient was estimated to be 7.5%, lead by the  $E_{tot}$  calibration uncertainty, by the low statistics at the spectra edge leading to uncertainties in the identification and matching of the *PM* and  $E_{tot}$  edges and, eventually, by the uncertainty brought by the linearization of the scintillator response.

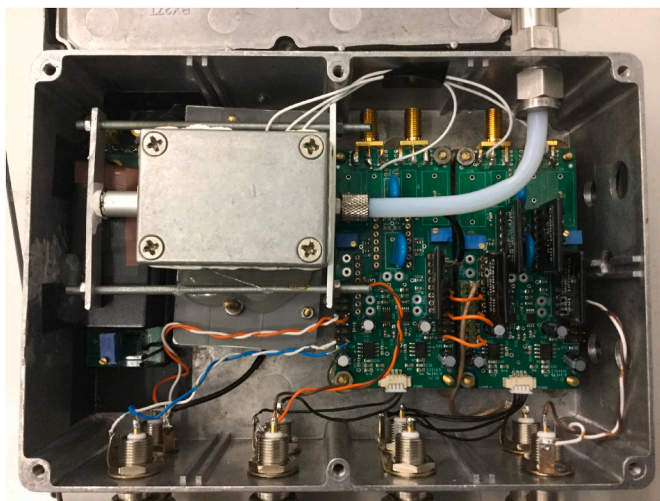


Fig. 2. Upper-view of the final ACSpect set up. The separation between the detectors region (left) and the front-end electronics region (right) is neat and visible.

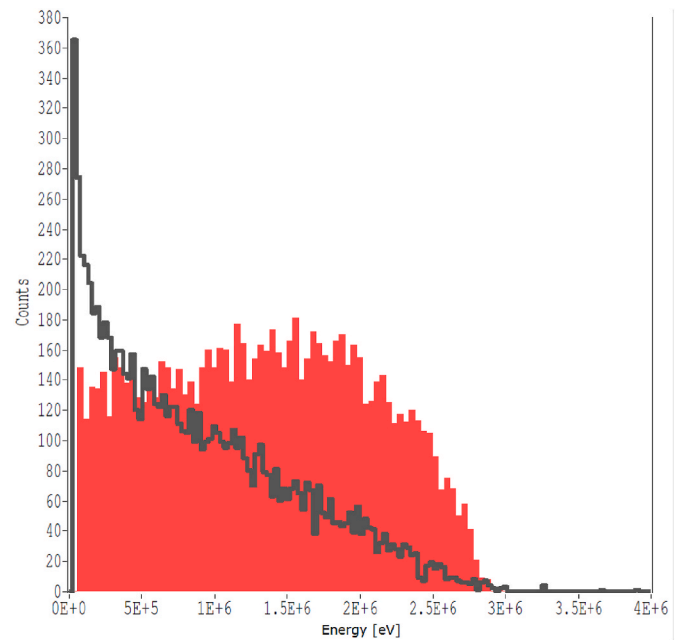


Fig. 3. Energy deposited by recoil-protons in the scintillator (grey spectrum) and in the  $E_{tot}$  stage of the telescope (red spectrum).

### 2.1.3. Data processing

A new elaboration program was implemented with LabVIEW™ (LabVIEW™.url), using a more appropriate algorithm for the recoil-proton selection and analysis.

In (n,p) scattering reactions, the neutron transfers its energy,  $E_n$ , to the recoil-proton according to the equation:

$$E_p = E_n \cos^2 \theta \quad (1)$$

where  $E_p$  is the recoil-proton energy,  $E_n$  is the neutron energy and  $\theta$  is the angle between the proton emission-direction and the neutron direction before the collision. Thanks to the collimator, all measured protons are directed within an angle  $\theta = 7.35^\circ$  with respect to the impinging neutrons. This allows to consider  $E_n \approx E_p$  with an uncertainty of about 1.63% (Stefano Agosteo et al., 2016). Hence, unfolding techniques are not required. This allows to compute on-line neutron spectrum while performing measurements. Once neutrons enter the converter, they can produce (n, p) scattering reactions with H atoms. Neglecting the nuclear reactions with  $^{12}\text{C}$  nuclei (which is a good approximation for neutron energies below 8 MeV), if  $n_0$  is the number of neutrons entering the converter and  $\Sigma_{np}$  is the (n, p) reaction cross section in polyvinyl-toluene, assuming the (n, p) scattering is the only interaction, the number of neutrons surviving a certain thickness  $t$  of the converter is  $n_{surv}(t) = n_0 e^{-\Sigma_{np} t}$ . The number of recoil protons  $p$  generated in a certain distance  $dx$  is  $p_{gen} = n_0 \Sigma_{np} dx$ . To reach the MST, the recoil-proton has to get out of the scintillator without being auto-absorbed. This means that it has to be generated within its range from the scintillator end. If  $t_{scint}$  is the polyvinyl-toluene scintillator thickness,  $R_p$  the proton range in polyvinyl-toluene, assuming  $\Sigma_{np}$  uniform within the scintillator but still depending on neutron energy, the number of detected protons  $p_{detected}$  is:

$$p_{detected} = n \left[ e^{-\Sigma_{np}(t_{scint}-R_p)} \Sigma_{np} R_p \varepsilon_{scint-MST} \right] \quad (2)$$

where  $\varepsilon_{scint-MST}$  is the efficiency with which a recoil-proton getting out of the scintillator reaches the MST through the collimator.  $\varepsilon_{scint-MST}$  was calculated by considering the geometry and the probability distribution of the recoil angle (Stefano Agosteo et al., 2016).

In order to couple the three output signals and discriminate proton

events from others, a *scatter plot* selection firstly picks out all those MST events within a proper range around the theoretical curve, Fig. 4. Distinguishing recoil-protons from secondary electrons generated in the silicon telescope by background photons is increasingly difficult for lower energies. In the ACSpect case, electrons are further discriminated from same-energy protons because electron events have not any corresponding *PM* signal. However, it could happen that some *PM*  $\gamma$  event or disturbance randomly occurs in time coincidence with the electron. An energy threshold of 40 keV is therefore set on both  $\Delta E$  and  $E_{tot}$ . To support the scatter plot selection, a time coincidence selection is performed on the two MST channels. The aim of this time coincidence is to further clean the signal from possible random disturbances or fake events.

A second, more important, time coincidence is performed between the  $\Delta E$  and *PM* signals. This allows to couple scintillator and MST events, discriminating recoil-protons in the *PM* at the same time. Fig. 5 shows the *PM* - $\Delta E$  time coincidence plot. The curve shape can be explained considering that *PM* signals have very narrow shapes as they are very fast signals. The trigger point (the point where the signal exceeds the trigger level) which determines the signal time-reference will not change much with the signal amplitude in the *PM*. For what concerns the  $\Delta E$  instead, which has a broader signal shape as it is slower, for lower amplitudes the signal slope is lower, and the trigger threshold is reached farther leading to a bigger delay between the two signals.

The linearization of the scintillator signal is performed using the algorithm described in (Stefano Agosteo et al., 2016), and the recoil-proton energy is finally achieved summing up the energies of the coupled events measured by scintillator and MST.

A data-acquisition program, based on the elaboration algorithm, was developed as well. It communicates with a Picoscope multi-channel analyser and it can provide a first on-line fast elaboration while saving all triggered signals. It prints out the measured neutron spectrum and allows to monitor each channel waveform and acquired spectrum. These on-line monitoring features are extremely useful in experimental contexts as they allow any problem to be identified and troubleshot while performing the measurement.

#### 2.1.4. Uncertainty analysis

The uncertainty of the neutron spectrum is calculated through a Monte Carlo calculation considering the counting statistics (uncertainty of type A) and the calibration factors uncertainties (type B). The input

quantity is the non-calibrated proton spectrum. A high enough number of proton spectra are randomly generated by sampling the yield in each energy bin from a Poisson function, whose mean value is the measured number of counts. For each of those spectra, the calibration coefficients are randomly generated too, by considering a uniform distribution. Related neutron spectra are calculated. Eventually, for each energy bin, the mean of all yield values generated, and the standard deviation are computed, providing the final neutron spectrum and associated uncertainties.

Additional type B uncertainties are finally added according to Taylor's error propagation (Taylor and McGuire, Second, 1997). These include:

- ACSpect distance from the source;
- integral accelerator charge used for the measurement or measurement time;
- sensitive detection area,  $\varepsilon = 2\%$ ;
- distance between ACSpect box and the scintillator,  $\sigma = 0.02$  mm.

While the first two items depend on how they are measured during the experiment, the last two have been assessed, being part of the instrument assembly, and their uncertainty values are indeed reported.

#### 2.2. Experimental campaign

The ACSpect was used for characterising the neutron field emerging from a beryllium target irradiated with protons. Measurements were carried out at the National Laboratories of Legnaro (LNL-INFN), Padua, Italy. The Van de Graaff CN accelerator was set-up to provide a 5 MeV proton beam impinging on a thick beryllium target. Both ACSpect and DIAMON were employed. Measurements were carried out with free-beam and with elements of neutron moderator. This was made of bricks of  $\text{AlF}_3$  added with lithium (3% in weight), a material that was proven as the best moderator to obtain an epithermal neutron beam for Boron Neutron Capture Therapy of deep-seated tumours (Ian Postuma et al., 2021).

The  $\text{AlF}_3$  tiles, shown in Fig. 6a, were produced by an innovative sintering process at the mechanical workshop of the INFN, Unit of Pavia, Italy.

Fig. 6b shows a picture of the experimental set-up used for measurements carried out using the ACSpect. The spectrometer and its

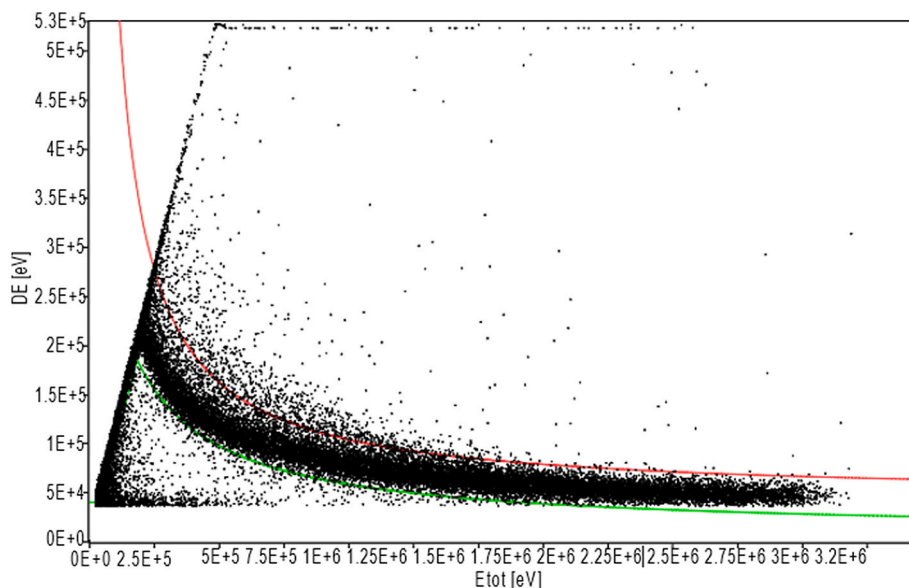


Fig. 4. Scatter plot of the events measured from an accelerator based neutron fluence at INFN LNL (the red and the green curves are the scatter plot selection curves). The  $\Delta E$  stage is referred to as *DE* in the figure.



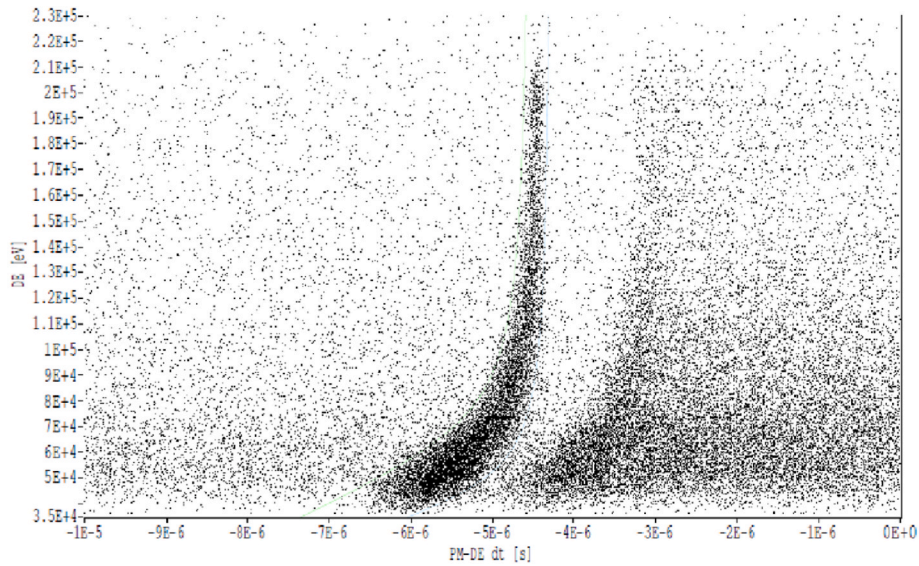


Fig. 5. Time coincidence plot between the PM and the  $\Delta E$  (DE in the figure) signals.

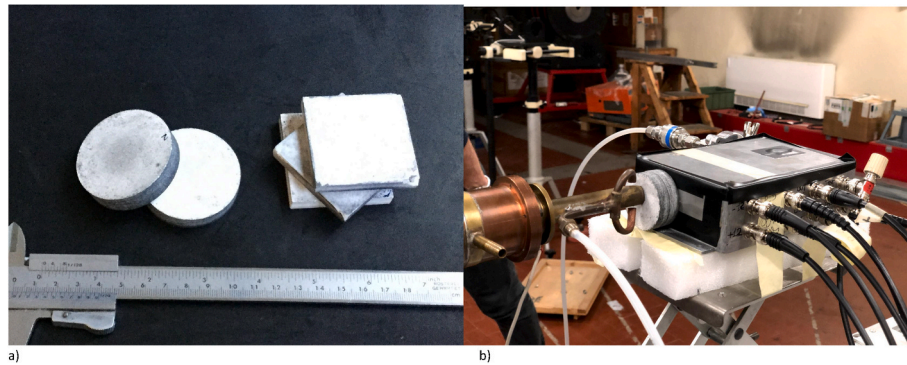


Fig. 6. a)  $AlF_3$  tiles used in the experiments at LNL. b) Picture of the ACSpect experimental set-up at LNL. From left to right, the beam exit and beryllium target, two  $AlF_3$  tiles and the ACSpect can be observed.

acquisition equipment were placed in the experimental room and remotely controlled from the control room. The beryllium target was equipped with a Faraday cup connected to an integral charge counter in order to monitor the quantity of protons delivered by the accelerator to the target.

The average proton current from the accelerator was about 40 nA.

### 2.2.1. DIAMON measurements

The DIAMON was placed at 130 cm from the beryllium target and centered at the  $0^\circ$  direction with respect to the beam-line, while the moderator was placed 2 cm downstream of the beryllium target. Measurements were carried out without and with three different  $AlF_3$  thicknesses: 2.16 mm, 4.47 mm and 6.63 mm. Three sets of measurements were performed for each configuration.

### 2.2.2. ACSpect experiments

The ACSpect was placed as close as possible to the beryllium target to have the highest achievable counting rate. The spectrometer was aligned with the beam-line and placed at 2.16 cm downstream of the beryllium target, thus allowing to position the 2.16 cm thick moderator in between during the second irradiation. The experiment and the ACSpect set-up are summarized in Table 1. A stabilized voltage generator was used to provide the  $\pm 12$  V supply and two different series of batteries provided the two bias-voltages. The acquisition device (PicoScope-4424) was connected to a PC running the acquisition program. A vacuum-pump

Table 1

ACSpect set-up and experiment set-up.

Power supply	$\pm 12$ V		
$p$ + bias	$-5.6$ V		
$E$ bias	142 V		
Vacuum pressure	$1.60 \times 10^{-1}$ mbar		
$AlF_3$ thickness	None	1.15 cm	2.16 cm
$Be_{target}$ - $AlF_3$ distance	-	0	0
$Be_{target}$ - ACSpect distance	2.16 cm	2.16 cm	2.16 cm

was used to put the MST and the collimator under vacuum.

### 2.3. Monte Carlo simulations

Monte Carlo simulations were carried out to be validated against the experimental measurements, so to obtain a reliable model for future calculations. Simulations were performed with the MCNP6 code.

Both the ACSpect and DIAMON experimental set-up were simulated. For what concern the ACSpect simulations, the contribution of the scattered neutrons can be neglected due to the short distance between the beryllium target and the detector and to the small sensitive area. Hence, a simplified geometry was implemented. The scoring region reproduces the shape and dimensions of the ACSpect sensitive volume and the moderator tiles are modelled as well. To save computational time, however, only a truncated-conical region filled with air and including

the scoring volume is left as the surrounding environment, as shown in Fig. 7. Air and lithiated  $\text{AlF}_3$ , which properties are listed in Table 2, are the only simulated materials.

For DIAMON set-up, the distance between the beryllium target and the detector is significantly higher (130 cm) and the scattered neutrons contribution is no longer negligible. However, since the scattered component was excluded from measurements results by performing twin-measurements with a shadow-cone during the experiments, a similar simplification of the simulation geometry was applied.

Variance reduction techniques were used in order to further improve calculation times. The neutron source was simulated using the double differential neutron spectra produced by the same reaction on beryllium, measured by Agosteo et al. (Stefano Agosteo et al., 2011) with the previous version of the ACSpect, at several angles with respect to the beam direction. Since the sensitive area of the ACSpect is small compared to the target, the simulation of a point-like source could be questionable. However, a further simulation demonstrated that the spectra obtained by sampling the neutron in a 1 cm diameter disk were not significantly different than those obtained with point-like approximation. The scoring quantity was the neutron fluence (MCNP f4 tally type) averaged over the sensitive volume and divided into uniformly distributed energy bins.

### 3. Results and discussion

The neutron energy spectra and the related integrals for different moderation thicknesses are presented below. These results are the first experimental neutron spectra obtained by moderation with solid  $\text{AlF}_3$ .

#### 3.1. Neutron energy spectra

The ACSpect demonstrated to be able to reconstruct neutron spectra with a satisfactory accuracy. Due to beam source instability and the related current limitations during the experimental campaign, the uncertainty due to the counting statistics was limited to about 10%. Uncertainties values of 0.1  $\mu\text{C}$  and 1 mm were assumed for the integral

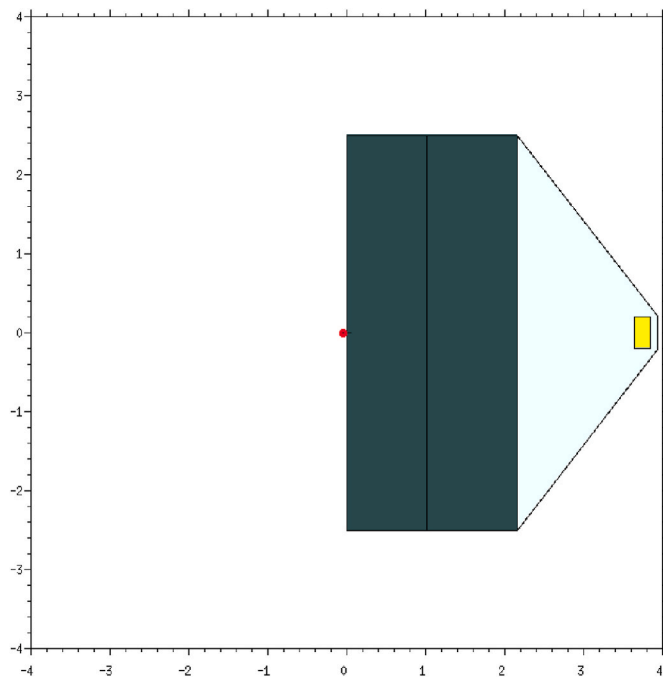


Fig. 7. Geometry configurations with two moderator tiles. The  $\text{AlF}_3$  is colored in grey, air is colored in light blue and tallies are yellow. The red dot at the beginning of the moderator is the point-like source position. Scale units are in cm.

Table 2

Compositions and density of the  $\text{AlF}_3$  tiles used in the experiments.

Lithiated $\text{AlF}_3$	
Element	Weight fraction [%]
$^{27}\text{Al}$	30.88
$^{19}\text{F}$	66.6
$^6\text{Li}$	0.189
$^7\text{Li}$	2.331
density [ $\text{g}/\text{cm}^3$ ]	2.5

beam charge and the distance between the spectrometer and the beryllium target respectively. The minimum detectable neutron energy was about 100 keV. Energy resolution (in terms of bins width) was 60 keV for energies lower than 400 keV and 40 keV for higher energies. However, results for energy below 200 keV have to be taken with care since at these low energies any non-idealities of the different stages of the spectrometer, in particular the scintillator interface, could affect the assessment of the proton energy because of its very high stopping power. Moreover, the system capability of discriminating between recoil protons and secondary electrons due to gammas could not be 100% effective. Nevertheless, below 250 keV there are no published experimental data for comparison.

Fig. 8 shows the comparison between the measurement performed without any moderator and the two other results reported in literature for the same irradiation field: Howard et al. (2001) by means of a *time of flight* system and by Agosteo et al. (Stefano Agosteo et al., 2011) by means of the first version of the ACSpect. Spectra well agree within uncertainties for energies higher than 600 keV. However, the region below 600 keV shows some discrepancies with both ToF and measurements from Agosteo et al. (Stefano Agosteo et al., 2011) with the same detector. This behaviour has to be investigated by further measurements and will be matter of future work.

Fig. 9 shows, instead, the three experimental spectra measured by the ACSpect. As expected, the spectrum undergoes an overall decrease with a slight shift towards lower energies. However, an appreciable peak shift cannot be observed from this first set of measurements, since only small moderator thicknesses could be used because of the low detection efficiency and low beam current. Further measurements to better investigate the new material moderation properties are planned for the future.

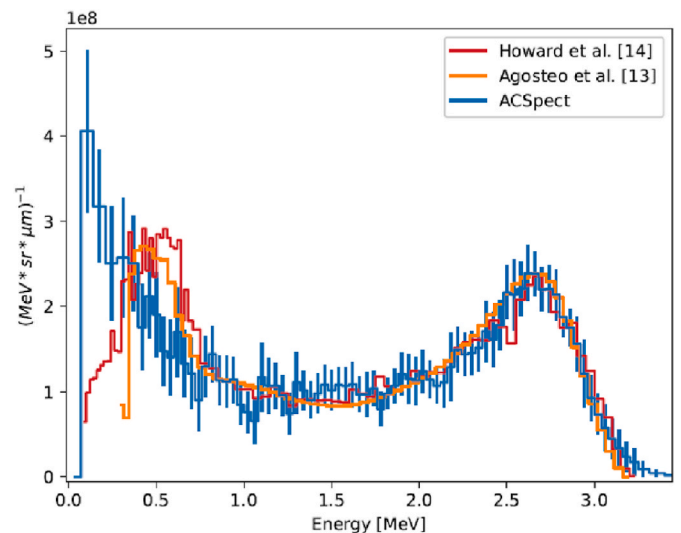


Fig. 8. Comparison between the neutron spectrum measured without moderator by the ACSpect, by Howard et al. (Howard et al., 2001) (Time Of Light) and by Agosteo et al. (Stefano Agosteo et al., 2011).

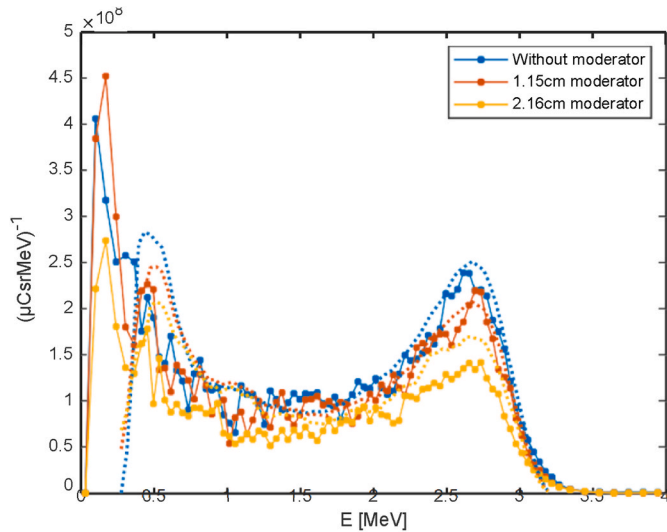


Fig. 9. Neutron spectra measured with the ACSpect at the CN accelerator of INFN's LNL. Solid line represents experimental measurements while dashed lines represent related simulations.

### 3.2. Neutron integral fluence

The total neutron fluence was also calculated by integrating the spectral distributions from the different detectors and simulated data for comparison. The spectra derived by DIAMON spectrometer are shown in Fig. 10. The spectra refer to the direct component of the neutron fields derived by adopting the ISO shadow cone method for the removal of the scattered components. It can be observed that for increasing moderator thicknesses, the spectrum shifts towards epithermal energy as expected. Table 3 lists the integral fluences measured by the two different detection systems, DIAMON and ACSpect, together with the results of simulations. All results are in good agreement and integral values resulted to be within uncertainties at each position and with every AlF<sub>3</sub> moderator thickness, thus proving the ACSpect reliability. A systematic overestimation of the integral fluence calculated by simulations is observed with respect of measured fluence. The reason behind this systematic overestimation could be the use of neutron energy spectra measured in a previous experiment, (Stefano Agosteo et al., 2011), to simulate the neutron beam delivered by the accelerator. Despite the same neutron

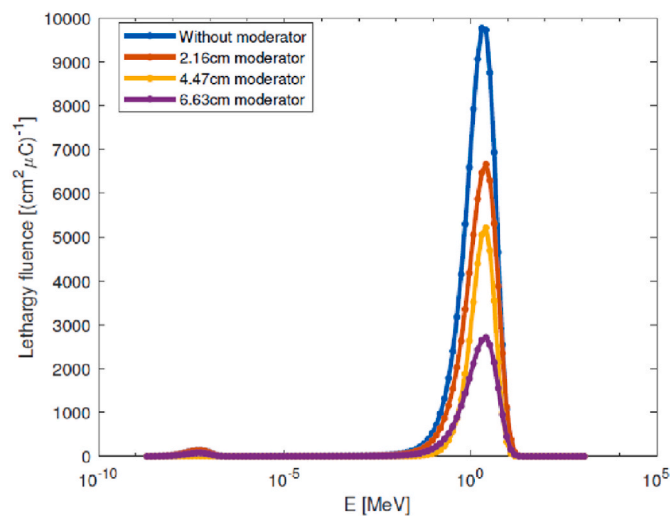


Fig. 10. Neutron spectra measured by DIAMON. All measurements are performed at 130 cm from the beryllium target. Neutron yields is in lethargy fluence units [ $\mu\text{C}^{-1} \text{cm}^{-2}$ ].

Table 3

Neutron integral fluence measured at LNL and calculated by means of Monte Carlo simulations, using different moderator thickness.

AlF <sub>3</sub>	Integral fluence [ $10^8 \mu\text{C}^{-1} \text{sr}^{-1}$ ]			
	DIAMON		ACSpect	
thickness [cm]	Experiments	Simulations	Experiments	Simulations
0	$3.93 \pm 0.16$	$4.19 \pm 0.23$	$3.94 \pm 0.12$	$4.19 \pm 0.23$
1.15			$3.51 \pm 0.10$	$3.83 \pm 0.21$
2.16	$2.73 \pm 0.11$	$3.18 \pm 0.11$	$2.6 \pm 0.07$	$3.35 \pm 0.18$
4.47	$1.66 \pm 0.07$	$1.87 \pm 0.07$		
6.63	$1.15 \pm 0.05$	$1.10 \pm 0.04$		

field in the same facility was measured during the experiment described in this work and by (Stefano Agosteo et al., 2011), indeed, the fluence today is expected to be lower than in the past, since the beryllium target had been used and thus deteriorated. This fluence discrepancy would then reflect on all the simulations carried out, giving rise to the systematic overestimation observed. Fig. 11 shows the integral fluence as a function of the AlF<sub>3</sub> moderator thickness. The overall attenuation coefficient  $\Sigma$  can be estimated by fitting measured values with an exponential function, hence assuming that the neutron fluence  $\Phi$  attenuates according to:  $\frac{\Phi(x)}{\Phi_0} = e^{-\Sigma x}$ , where  $x$  is the path-length flown in the moderator and  $\Phi_0$  is the neutron fluence without moderator. The obtained values, reported in Table 4, further highlight the good agreement between the two spectrometers and with the simulations.

### 4. Conclusions

The ACSpect is an innovative high-resolution neutron spectrometer first implemented by the Nuclear Measurements group of the Energy department of Politecnico di Milano (Stefano Agosteo et al., 2007, 2016). This work presented the improvements performed by changing its technological configuration and the elaboration process: the spectrometer is now more compact, thus very easily transportable, and much less sensitive to external noise.

Experiments and Monte Carlo simulations were carried out to test the new-ACSpect characteristics in the frame of a wider experiment in which the properties of AlF<sub>3</sub> mixed with LiF are being characterised for BNCT applications. The densified material was produced in Pavia through an innovative sintering process and in-beam measurements had never been carried out before this work.

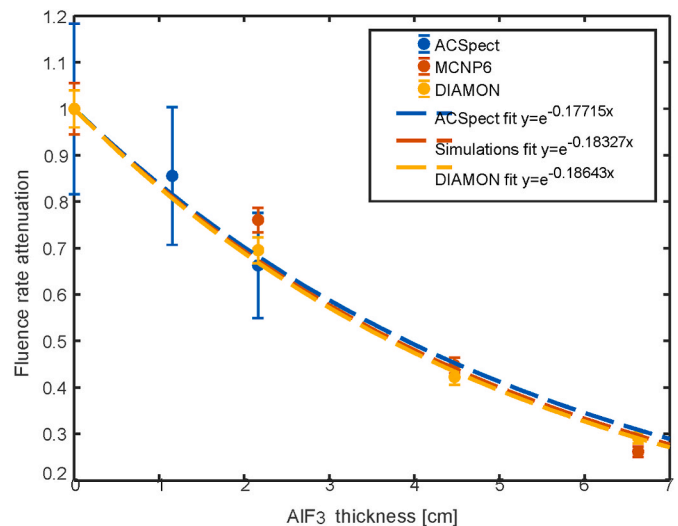


Fig. 11. Fluence rate attenuation plotted versus the AlF<sub>3</sub> thickness. Dashed curves are the respective exponential fits, whose related equations are reported on the legend together with the R<sup>2</sup> of the fit.



**Table 4**

Neutron fluence attenuation coefficient of  $\text{AlF}_3$ , in the energy range from about 200 keV to 3.2 MeV.

Attenuation coefficient [ $\text{cm}^{-1}$ ]	
DIAMON	$0.1864 \pm 0.0099(5.3\%)$
ACSpect	$0.1772 \pm 0.0143(8.1\%)$
Simulations	$0.1833 \pm 0.0118(6.4\%)$

Monte Carlo simulations were performed using the *MCNP6* Monte Carlo radiation transport code, which is considered the gold standard among the Monte Carlo codes concerning coupled neutron-photon-electron transport.

Experiments were carried out at the CN accelerator facility at the LNL of INFN. The neutron beam was obtained through the nuclear reaction  ${}^9\text{Be}(p,n){}^9\text{B}$  by delivering a 5 MeV proton beam on a beryllium target. Neutron spectra were measured by means of the ACSpect without any moderator, with 1.15 cm and with 2.16 cm-thick  $\text{AlF}_3$  bricks and compared to the Monte Carlo model for its validation. From the spectra, the integral neutron fluence was calculated and compared with the integral fluence measured by the DIAMON spectrometer. Results are in good agreement within their uncertainties. Eventually, the  $\text{AlF}_3$  neutron fluence attenuation coefficient was derived and found to be  $0.186 \pm 0.008 \text{ cm}^{-1}$ .

The optimised ACSpect proved to be a reliable, easy-to-use and compact system and allowed the reconstruction of neutron spectra with a good energy resolution. The energy resolution is 40 keV in the energy range between 250 keV and 4 MeV. Despite its promising results, before the ACSpect could be reliably applied to a clinical BNCT beam, two main challenges have to be overcome. A high fluence of about  $10^9 \text{ cm}^{-2} \text{ s}^{-1}$  is to be expected for a therapy intense neutron beam. Even though the scintillator is characterised by a very fast time response and its detection efficiency could be customised by properly sizing the scintillator, an improved and faster front-end electronics needs to be implemented for the scintillator to reliably operate at therapeutic fluence conditions. Further, the spectral distribution of a neutron beam suitable for BNCT of deep-seated tumours is peaked below the energy range measured by the ACSpect, whose low energy threshold should ideally be lowered to few keV. Nevertheless, the ACSpect proved to be a valuable instrument when designing and tailoring a neutron beam for BNCT, allowing a precise evaluation of the spectral changes due to the insertion of a moderator between the neutron source and the beam port.

The measurements are also the first experimental neutron spectra obtained with densified  $\text{AlF}_3$  added with LiF as moderator and offered a first validation of the Monte Carlo calculations involving this novel moderator material. However, Monte Carlo results showed a general overestimation of the experimental results. While the systematic overestimation can be attributed to an inaccurate (out of date) normalisation

of the neutron source modelled, the higher discrepancy found with 2.16 cm of moderator could be linked to inaccuracies in the cross sections employed by MCNP6 and pushed to further investigations.

Further work concerns new experimental measurements with different configurations of the moderator. The experimental results obtained with ACSpect and DIAMON will be used to validate the simulation of the neutron spectra which will be finally used for treatment planning computation.

### Declaration of competing interest

The authors declare that they have no known competing financial interests or personal relationships that could have appeared to influence the work reported in this paper.

### Acknowledgements

Funding: This work was partially funded by INFN (National Institute of Nuclear Physics), project BEAT\_PRO.

### References

- Howard, W.B., et al., 2001. Measurement of the thick-target  ${}^9\text{Be}(p,n)$  neutron energy spectra. *Nucl. Sci. Eng.* 145–160, 138.2.
- Ian Postuma, et al., 2021. A novel approach to design and evaluate BNCT neutron beams combining physical, radiobiological, and dosimetric figures of merit. *Biology*. <https://doi.org/10.3390/biology10030174>, 10.3. <https://www.mdpi.com/2079-7737/10/3/174>.
- John Bettely Birks, 1951. "Scintillations from organic crystals: specific fluorescence and relative response to different radiations. In: *Proceedings of the Physical Society*, A64.10.
- John Bettely Birks, 1964. *The theory and practice of scintillation counting*. In: Fry, D.W., Costrell, L., Kandiah, K. (Eds.), Pergamon.
- LabVIEW<sup>TM</sup>. <https://www.ni.com/en-gb/shop/labview.html>.
- Pola, A., et al., 2020. DIAMON: a portable, real-time and direction-aware neutron spectrometer for field characterization and dosimetry. *Nucl. Instrum. Methods Phys. Res.* 969.
- Rosenfeld, A.B., et al., 1999. A new detector for microdosimetry applications in proton therapy. In: *IEEE Nuclear Science Symposium And Medical Imaging Conference*, vol. 1, pp. 331–338.
- Saint-Gobain Crystals. Plastic product brochure. [http://www.crystals.saint-gobain.com/Plastic\\_Scintillators.aspx](http://www.crystals.saint-gobain.com/Plastic_Scintillators.aspx).
- Saint-Gobain Crystals. BC-404 scintillator. [http://www.crystals.saint-gobain.com/Plastic\\_Scintillators.aspx](http://www.crystals.saint-gobain.com/Plastic_Scintillators.aspx).
- Stefano Agosteo, et al., 2007. Neutron spectrometry with a monolithic silicon telescope. *Radiat. Protect. Dosim.* 126, 210–217.
- Stefano Agosteo, et al., 2011. "Characterization of the energy distribution of neutrons generated by 5 MeV protons on a thick beryllium target at different emission angles". *Appl. Radiat. Isot.* 69, 1664–1667.
- Stefano Agosteo, et al., 2016. A telescope detection system for direct and high resolution spectrometry of intense neutron fields. *Radiat. Meas.* 85, 1–17.
- Taylor, J.R., 1997. *An introduction to error analysis: the study of uncertainties in physical measurements*. In: McGuire Second, Ann (Ed.), University Science Books. <http://www.hamamatsu.com/eu/en/product/category/3100/3003/3044/H10720-110/index.html>.